ORIGINAL PAPER

Podocytes are new cellular targets of haemoglobin-mediated renal damage

Alfonso Rubio-Navarro[1], Maria Dolores Sanchez-Niño[1,2], Melania Guerrero-Hue[1], Cristina García-Caballero[1], Eduardo Gutiérrez[2,3], Claudia Yuste[2,3], Ángel Sevillano[2,3], Manuel Praga[2,3], Javier Egea[4,5], Elena Román[6], Pablo Cannata[2,7], Rosa Ortega[8], Isabel Cortegano[9], Belén de Andrés[9], María Luisa Gaspar[9], Susana Cadenas[10,11], Alberto Ortiz[1,2], Jesús Egido[1,12] and Juan Antonio Moreno[1]*

[1] Renal, Vascular and Diabetes Research Laboratory, Fundación Instituto de Investigación Sanitaria-Fundación Jiménez Díaz, Autónoma University, Madrid, Spain
[2] Red de Investigación Renal (REDINREN), Madrid, Spain
[3] Department of Nephrology, Hospital 12 de Octubre, Madrid, Spain
[4] Instituto de Investigación Sanitaria-Hospital Universitario de la Princesa, Madrid, Spain
[5] Instituto Teófilo Hernando, Department of Pharmacology and Therapeutics, Medicine Faculty, Autónoma University, Madrid, Spain
[6] Paediatric Nephrology Department, La Fe Hospital, Valencia, Spain
[7] Pathology Department, Fundación Instituto de Investigaciones Sanitarias-Fundación Jiménez Díaz, Autónoma University, Madrid, Spain
[8] Pathology Department, Hospital Universitario Reina Sofia, Córdoba, Spain
[9] Immunology Department, Centro Nacional de Microbiología, Instituto de Salud Carlos III (ISCIII), Madrid, Spain
[10] Centro de Biología Molecular 'Severo Ochoa' and Molecular Biology Department, Autónoma University, Madrid, Spain
[11] Instituto de Investigación Sanitaria La Princesa, Madrid, Spain
[12] Spanish Biomedical Research Centre in Diabetes and Associated Metabolic Disorders (CIBERDEM), Madrid, Spain

*Correspondence to: J Antonio Moreno, Vascular, Renal and Diabetes Research, IIS-Fundación Jiménez Díaz, Av. Reyes Católicos 2, 28040 Madrid, Spain. E-mail: jamoreno@fjd.es

Abstract

Recurrent and massive intravascular haemolysis induces proteinuria, glomerulosclerosis, and progressive impairment of renal function, suggesting podocyte injury. However, the effects of haemoglobin (Hb) on podocytes remain unexplored. Our results show that cultured human podocytes or podocytes isolated from murine glomeruli bound and endocytosed Hb through the megalin–cubilin receptor system, thus resulting in increased intracellular Hb catabolism, oxidative stress, activation of the intrinsic apoptosis pathway, and altered podocyte morphology, with decreased expression of the slit diaphragm proteins nephrin and synaptopodin. Hb uptake activated nuclear factor erythroid-2-related factor 2 (Nrf2) and induced expression of the Nrf2-related antioxidant proteins haem oxygenase-1 (HO-1) and ferritin. Nrf2 activation and Hb staining was observed in podocytes of mice with intravascular haemolysis. These mice developed proteinuria and showed podocyte injury, characterized by foot process effacement, decreased synaptopodin and nephrin expression, and podocyte apoptosis. These pathological effects were enhanced in Nrf2-deficient mice, whereas Nrf2 activation with sulphoraphane protected podocytes against Hb toxicity both *in vivo* and *in vitro*. Supporting the translational significance of our findings, we observed podocyte damage and podocytes stained for Hb, HO-1, ferritin and phosphorylated Nrf2 in renal sections and urinary sediments of patients with massive intravascular haemolysis, such as atypical haemolytic uraemic syndrome and paroxysmal nocturnal haemoglobinuria. In conclusion, podocytes take up Hb both *in vitro* and during intravascular haemolysis, promoting oxidative stress, podocyte dysfunction, and apoptosis. Nrf2 may be a potential therapeutic target to prevent loss of renal function in patients with intravascular haemolysis.
Copyright © 2017 Pathological Society of Great Britain and Ireland. Published by John Wiley & Sons, Ltd.

Keywords: intravascular haemolysis; haemoglobin; podocyte; oxidative stress; apoptosis; Nrf2

Introduction

Free haemoglobin (Hb) is nephrotoxic, promoting acute kidney injury (AKI) and contributing to the progression of chronic kidney disease [1,2]. Renal Hb overload is the pathophysiological consequence of recurrent and massive intravascular haemolysis, as reported in many hereditary and immune diseases, including sickle cell disease (SCD), atypical haemolytic uraemic syndrome (aHUS), and paroxysmal nocturnal haemoglobinuria (PNH), among others [3].

Destruction of erythrocytes releases free Hb into plasma, where it rapidly binds haptoglobin (Hp) to form a highly stable Hb–Hp complex that is degraded by the liver, spleen, and bone marrow, avoiding glomerular filtration of Hb. However, persistent intravascular

haemolysis depletes plasma Hp, allowing free Hb to be filtered by glomeruli and incorporated into proximal tubules through the megalin−cubilin receptor system [4]. Intracellular Hb dissociates into globin and haem. Haem oxygenase-1 (HO-1) catalyses the conversion of haem to biliverdin and carbon monoxide, a reaction yielding iron, which is subsequently stored in ferritin [5]. Therefore, the HO-1−ferritin axis minimizes cellular exposure to haem and catalytically active 'free' iron [6]. The renal toxicity of Hb is associated with increased oxidative stress, apoptosis, and inflammation [4]. Nuclear factor erythroid-2-related factor 2 (Nrf2) plays a central role in the defence against Hb-mediated oxidative stress by activating the expression of >250 antioxidants and phase 2 detoxifying enzymes and related proteins, including HO-1 [7].

Renal tubules are considered to be the main sites of Hb nephrotoxicity. However, proteinuria is observed in experimental models of recurrent exposure to haem proteins [8], and focal segmental glomerulosclerosis develops in experimental SCD [9] and in patients with chronic and recurrent haemolysis, such as aHUS, PNH, or SCD [10,11], who may develop proteinuria [12,13] and a chronic decrease in glomerular filtration [2,14]. These data suggest a link between chronic intravascular hemolysis and glomerular dysfunction. However, the pathophysiological mechanisms remain unclear. Haemodynamic changes were suggested to promote proteinuria and progressive renal damage in SCD [15]; however, there is no definitive proof of this hypothesis. As focal segmental glomerulosclerosis implies a loss of podocytes, additional factors that directly injure podocytes may play a role.

Podocytes are highly differentiated epithelial cells that play a key role in preserving glomerular filtration barrier integrity [16]. Podocyte foot processes prevent the urinary leakage of plasma proteins [17]. Thus, podocyte injury or loss lead to proteinuria [18]. Although podocyte damage and podocyturia have been described in haemolytic diseases [19,20], and iron-containing deposits are observed in podocytes [21], the effects of Hb on podocytes remain unexplored. We hypothesized that Hb trafficking across the glomerular filtration barrier may injure podocytes, and thereby impair glomerular permselectivity in patients with persistent intravascular haemolysis, contributing to renal disease progression. In support of this hypothesis, the megalin−cubilin receptor system, which is involved in Hb uptake by tubular cells, is also expressed in human podocytes [22,23]. Thus, we investigated whether Hb is incorporated into podocytes *in vitro*, and can be detected in kidney biopsies and urinary sediments from patients with severe intravascular haemolysis. To further clarify the role of Hb in podocyte injury, we analysed oxidative stress, apoptosis and structural changes *in vitro* and in a murine model of intravascular haemolysis by using wild-type and Nrf2-deficient mice. Finally, we also examined the molecular pathways involved in Hb-mediated podocyte injury, and explored whether podocyte damage is prevented by activation of Nrf2 *in vivo*.

Materials and methods

In vitro studies

Human podocytes (kindly provided by MA Saleem, Bristol, UK) are immortalized cells, transfected with a temperature-sensitive SV40 gene construct and a gene encoding the catalytic domain of human telomerase, as described previously [24]. These cells were cultured in RPMI-1640 medium with penicillin, streptomycin, insulin, transferrin, selenite and 10% fetal bovine serum at a permissive temperature of 33 °C, remaining in an undifferentiated proliferative state. Once cells reached 70−80% confluence, they were cultured at 37 °C for 14 days to induce differentiation [24]. Expression of the podocyte markers nephrin and synaptopodin was used to ensure its identity.

For uptake studies, human Hb (HbAo; Sigma-Aldrich, St Louis, MO, USA) or mouse Hb (CSB-NP004901m; Cusabio, College Park, MA, USA) were labelled with an Alexa-488 labelling kit (Life Technologies, Carlsbad, CA, USA). Podocytes were incubated for 2 h with labelled Hb, and Hb uptake was quantified with a FacsCanto II flow cytometer (BD Biosciences, San Jose, CA, USA).

Hypodiploid and apoptotic cells were counted by flow cytometry with propidium iodide staining and a Annexin V/7AAD Apoptosis Detection Kit (BD Biosciences), respectively. Mitochondrial membrane potential was quantified by flow cytometry with a tetramethyl rhodamine methylester (TMRM) fluorescent probe (Invitrogen, Carsbad, CA, USA).

The molecular probe $2',7'$-dichlorodihydrofluorescein diacetate (H_2DCFDA) (C6827; Invitrogen) was used for measurement of intracellular reactive oxygen species (ROS). NADPH oxidase-dependent ROS production was assessed with a lucigenin-enhanced chemiluminescence assay [25]. Dihydroethidium (DHE) (Invitrogen) was used to evaluate *in situ* production of superoxide anion [25]. Monochlorobimane was used to quantify reduced glutathione (GSH) [26]. HO-1 activity in microsomal fractions from podocytes was quantified spectrophometrically by measurement of bilirubin production [27].

Animal experiments

Animal studies were performed in accordance with Directive 2010/63/EU of the European Parliament, and were approved by the Institutional Animal Care and Use Committee (IIS-Fundacion Jimenez Diaz).

Haemolysis was induced in 12-week-old C57BL/6 mice or Nrf2-deficient mice (obtained from S. Cadenas, Spain) by intraperitoneal administration of phenylhydrazine (Phe) (200 mg/kg body weight; Sigma-Aldrich). Sulphoraphane (Sfn) (12.5 mg/kg body weight; Cayman

Table 1. Clinical characteristics and haematological parameters of patients with AKI-associated haemolytic anaemia

	aHUS (microangiopathic haemolytic anaemia)		Haemolytic anaemia secondary to transfusion
	Case 1	Case 2	Case 3
Age (years)	23	56	47
Gender	Female	Female	Male
Creatinine (mg/dl)	6.8	2	8
Hb (g/dl)	7.2	10.9	6.8
Platelets/µl	62 000	45 000	–
Hp (mg/dl)	2	<1	–
LDH (IU/l)	6760	1979	1800

LDH, lactate dehydrogenase.

Chemical, Ann Arbor, MI, USA) was administered intraperitoneally 48, 24 and 2 h before Phe injection. Mice were killed 24 h after Phe injection, and blood and urine samples were collected for biochemical analysis (ADVIA 2400 Clinical Chemistry System; Siemens Healthcare, Erlangen, Germany) and haematological analysis (Scil Vet ABC haematology analyser; Scil, Madrid, Spain). Dissected kidneys were fixed in 4% paraformaldehyde and embedded in paraffin (immuno-histochemistry/immunofluorescence), fixed with 1% glutaraldehyde and 4% formaldehyde, and further embedded in Durcupan resin for transmission electron microscopy, or snap-frozen for RNA and protein expression determination, as described previously [25,28,29]. To determine Hb uptake by murine podocytes, dissected kidneys were digested with 0.5 mg/ml collagenase (Sigma-Aldrich) and 50 U/ml DNase I (Roche, Basilea, Switzerland) in Hank's balanced salt solution at 37 °C for 20 min. Erythrocytes were lysed with a lysing buffer (A10492-01; Gibco, Grand Island, NY, USA). Renal cell suspensions were incubated with labelled Hb for 2 h at 37 °C, and further analysed by flow cytometry.

Human renal biopsies

We identified renal biopsies from one patient with haemolytic anaemia secondary to a severe transfusion reaction caused by the presence of anti-Kell antibodies in the transfused blood and from two patients with aHUS–AKI and microangiopathic haemolytic anaemia (Table 1). Patients gave informed consent, and the study was approved by the local Ethics Committee. Control samples were obtained from non-tumour renal tissue after surgery in patients with kidney cancer.

Real-time quantitative polymerase chain reaction (RT–qPCR)

Total RNA from kidneys or cultured cells was isolated with TriPure reagent (Roche), and reverse-transcribed with a High Capacity cDNA Archive Kit (Applied Biosystems, Foster City, CA, USA). Quantitative gene expression analysis was performed on an AB7500 fast real-time polymerase chain reaction system (Applied Biosystems) with Taqman gene expression assays (supplementary material, Table S1).

Protein studies

Proteins from renal tissues or cultured cells were isolated in lysis buffer and analysed by western blotting, as previously described [28]. Primary antibodies (supplementary material, Table S2) were detected with an appropriate horseradish peroxidase (HRP)-conjugated secondary antibody, developed by use of Luminata Crescendo Western HRP substrate (Millipore, Burlington, MA, USA), and scanned with an ImageQuant LAS-4000 (GE Healthcare, Little Chalfont, UK). Urinary levels of nephrin and albumin were determined by enzyme-linked immunosorbent assay (ELISA) [Exocell (Philadelphia, PA, USA) and Abcam (Cambridge, UK), respectively], and then normalized to urinary creatinine concentration (Creatinine Assay Kit; Abcam).

Immunofluorescence

Immunofluorescence studies were performed on paraffin-embedded kidney sections (3 µm), urine sediments, or cultured podocytes, as described previously [30]. Specific primary antibodies are listed in supplementary material, Table S2. Quantification of protein expression was performed on 30 glomeruli/mouse with Image-Pro Plus software (Media Cybernetics, Rockville, MD, USA), with similar acquisition settings in all tissues. Samples from each mouse were examined in a blinded manner.

Statistical analysis

In vitro data were expressed as mean ± standard deviation (SD), and *in vivo* data were expressed as mean ± standard error of the mean (SEM). Differences between groups were analysed with the Kruskall–Wallis test and the Mann–Whitney *U*-test. Pearson correlation analyses were performed for normally distributed parameters. *P* values of <0.05 were considered to be significant. Statistical analysis was performed with SPSS 11.0 statistical software (IBM, New York, NY, USA).

Results

Podocytes bind and endocytose Hb through the megalin–cubilin receptor system, promoting oxidative stress and podocyte dysfunction

To study whether Hb is incorporated into podocytes, we performed both flow cytometry and confocal microscopy studies with fluorescently labelled Hb. Concentration-dependent Hb uptake was observed in cultured human podocytes (Figure 1A, B; supplementary material, Figure S1A, B). Preincubation with unlabelled Hb decreased further uptake of fluorescent Hb, indicative of binding-dependent uptake (supplementary material, Figure S1C). Furthermore, Hb uptake at 4 °C was lower than at 37 °C, suggesting energy-dependent, active Hb uptake (supplementary material, Figure S1D). Similar results were obtained
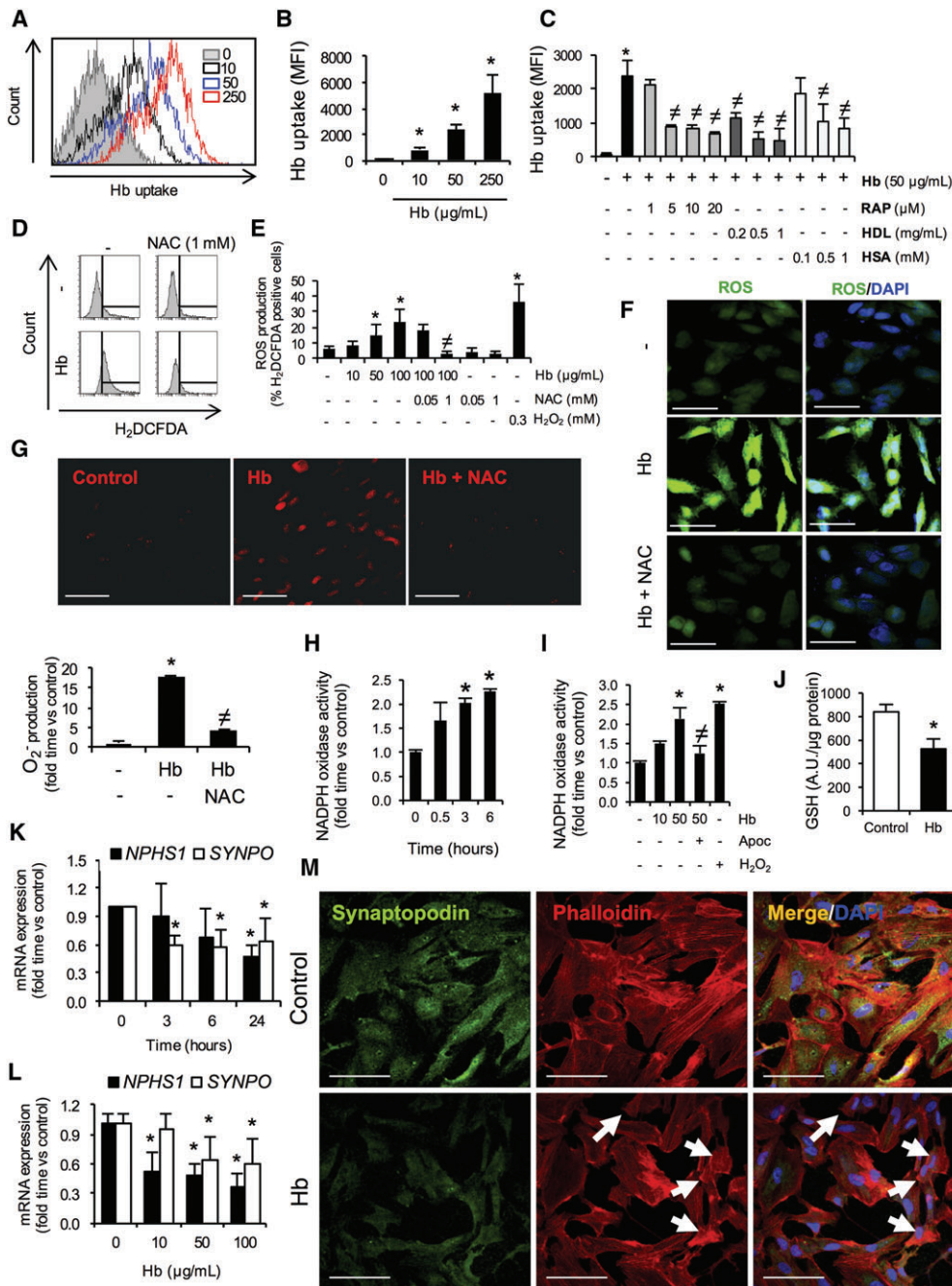
Figure 1. Hb uptake by podocytes is mediated by the megalin–cubilin system, and promotes oxidative stress and podocyte dysfunction. Human podocytes were cultured in serum-free medium, and incubated with different concentrations of Alexa Fluor 488-labelled haemoglobin (Hb) (10–250 µg/ml) for 2 h. After washing, Alexa Fluor 488–Hb uptake was determined by flow cytometry. (A and B) Representative histogram (A) and mean fluorescence intensity (MFI) quantification (B) showing fluorescence-labelled Hb uptake by podocytes. *$p < 0.05$ as compared with non-treated cells. (C) Inhibition of Alexa Fluor 488-Hb uptake (50 µg/ml) by pretreatment for 1 h with several megalin–cubilin antagonists, such as RAP (1–20 µM), HDL (0.2–1 mg/ml), or HSA (0.01–1 mM). ROS production was estimated by flow cytometry with the fluorescent dye H_2DCFDA (5 µM). (D and E) Representative H_2DCFDA fluorescence histograms (D) and ROS production quantification (E) in human podocytes incubated with different concentrations of Hb (10–100 µg/ml) for 3 h. Pretreatment for 1 h with NAC (1 mM) reduced oxidative stress. H_2O_2 (0.3 mM) was used as a positive control. (F) Representative confocal images showing ROS production (green) in podocytes stimulated with Hb for 3 h. Nuclei were stained with 4′,6-diamidino-2-phenylindole (DAPI) (blue). Scale bars: 50 µm. (G) Differentiated podocytes were treated with Hb and DHE for 3 h. After that, production of superoxide anion (DHE-derived fluorescence intensity) was determined by confocal microscopy (upper panel), and further quantified with Image-Pro plus software (lower panel). Scale bars: 100 µm. (H and I) NADPH oxidase activity was determined with a lucigenin-enhanced chemiluminescence assay in cells stimulated for 0–6 h with different Hb concentrations (10–50 µg/ml) in presence or absence of the antioxidant apocynin (Apoc) (100 µM). (J) Intracellular GSH content in podocytes treated with Hb (100 µg/ml) for 3 h. (K and L) Podocytes were stimulated with different Hb concentrations (0–100 µg/ml) for up to 24 h before analysis of *NPHS1* and *SYNPO* mRNA expression by RT-qPCR. (M) Representative immunofluorescence images showing synaptopodin (green) in podocytes stimulated with Hb for 24 h. Phalloidin (red) and DAPI (blue) were used to stain the actin cytoskeleton and nuclei, respectively. Arrows indicate round-shaped podocytes after Hb exposure. Note that actin filaments showed a pericellular distribution in podocytes stimulated with Hb. Scale bars: 100 µm. Results are expressed as mean ± SD of four independent experiments. *$p < 0.05$ versus non-treated cells; ≠$p < 0.05$ versus Hb-stimulated cells.

in podocytes isolated from murine glomeruli (supplementary material, Figure S2). As the megalin–cubilin receptor complex mediates Hb uptake in renal proximal tubules [4] and is expressed by podocytes [22,23], we assessed whether it contributed to Hb uptake in podocytes. Hb uptake was inhibited by receptor-associated protein (RAP), a specific inhibitor of the megalin–cubilin system, and by other ligands of these receptors, such as human serum albumin (HSA) and high-density lipoprotein (HDL) (Figure 1C), suggesting that this receptor system is involved in Hb uptake by podocytes.

We further determined the production of ROS in Hb-stimulated podocytes. Hb increased the production of both hydrogen peroxide and superoxide anion, an effect that was inhibited by the antioxidant *N*-acetylcysteine (NAC) (Figure 1D–G). NADPH oxidase is an enzymatic source of ROS that is highly expressed in podocytes [31]. Hb increased NADPH oxidase-mediated ROS production, an effect that was partially inhibited by the antioxidant apocynin (Figure 1H, I). Oxidative stress results from an imbalance between increased ROS production and reduced antioxidant defences. Therefore, we determined the effect of Hb on GSH, the most abundant endogenous antioxidant [32]. Hb reduced GSH levels in podocytes (Figure 1J), indicating that Hb-mediated oxidative stress results from both increased ROS production and reduced intracellular antioxidant defences.

The slit diaphragm proteins nephrin and synaptopodin play a key role in maintaining normal podocyte ultrastructure and function, and are biomarkers of podocyte injury [33]. In cultured podocytes, Hb decreased nephrin (*NPHS1*) and synaptopodin (*SYNPO*) mRNA expression in a time-dependent and dose-dependent manner (Figure 1K, L). Confocal microscopy confirmed the decreased expression of synaptopodin in Hb-stimulated podocytes (Figure 1M). These cells showed a more rounded shape and disorganization of actin filaments, with a perinuclear distribution, as compared with non-treated cells, suggesting an altered cytoskeletal architecture in response to Hb.

Hb promotes apoptosis in cultured podocytes

ROS may induce podocyte apoptosis [34], so we explored Hb-mediated apoptosis in podocytes. Hb augmented the number of hypodiploid apoptotic podocytes in a concentration-dependent manner (Figure 2A). Staining with 7-aminoactinomycin D (7-AAD)/annexin V confirmed the increase in the percentage of apoptotic cells (Figure 2B). Moreover, Hb reduced the number of attached podocytes, and promoted nuclear condensation and cell shrinkage, which are features associated with apoptosis (Figure 2C). We further explored the molecular pathways of apoptosis induced by Hb. Hb increased proapoptotic Bax levels and decreased anti-apoptotic BclxL levels, resulting in an increased Bax/BclxL ratio (Figure 2D). Hb also promoted loss of mitochondrial membrane potential and subsequent cytochrome *c* redistribution from mitochondria to the cytoplasm (Figure 2E, F). Cytochrome *c* release activates the apoptosome and caspases [35]. Pretreatment with zVAD, a pan-caspase inhibitor, prevented Hb-induced apoptosis, indicating the involvement of caspases in Hb-mediated cell death (Figure 2C). Moreover, exposure to Hb activated caspase-3, the central executioner caspase, and resulted in cleavage of poly-ADP-ribose-polymerase-1 (PARP-1), a caspase-3 substrate that is necessary for cellular survival [36] (Figure 2G). Altogether, these results show activation of the intrinsic apoptosis pathway in Hb-stimulated podocytes.

Hb induces Nrf2–HO-1 signalling in podocytes

Hb activated Nrf2 in podocytes, as shown by nuclear translocation of this transcription factor (Figure 3A, B). Nuclear Nrf2 regulates the transcription of phase II antioxidant enzymes, including HO-1, which degrades intracellular haem [5]. Hb induced a time-dependent and concentration-dependent increase in HO-1 (*HMOX1*) mRNA and protein expression, as well as an increase in HO-1 activity (Figure 3C, D; supplementary material, Figure S3A–D). Similar results were obtained for other Nrf2-responsive genes (supplementary material, Figure S3D). Nrf2 (*NFE2L2*) targeting with specific small interfering RNAs (siRNAs) partially reduced Hb-mediated *HMOX1* induction, suggesting the existence of alternative pathways that regulate HO-1 expression (Figure 3E). Also, restoring GSH levels with the antioxidant NAC also reduced Hb-induced HO-1 protein and mRNA expression (Figure 3E, F). HO-1 may be induced by a number of oxidant stimuli [37]. To verify whether Hb-mediated HO-1 induction was directly associated with haem catabolism, we determined ferritin expression. Ferritin is directly associated with HO-1 activity, because it is the enzyme that stores free iron released from haem by HO-1 [38]. Ferritin expression was increased in Hb-stimulated podocytes (Figure 3C, G; supplementary material, Figure S3A, B), an effect that was abrogated by the HO-1 inhibitor tin protoporphyrin IX (SnPP) (Figure 3G). These results show that Hb activates Nrf2 and induces the expression of metabolically active HO-1, which promotes ferritin expression to decrease the levels of intracellular Hb derivatives resulting from Hb uptake in podocytes.

Next, we studied whether effective Nrf2 or HO-1 targeting may prevent Hb toxicity (Figure 3H). Nrf2 and HO-1 disruption by specific siRNAs or pre-stimulation with the HO-1 inhibitor SnPP enhanced Hb-mediated ROS production, increased depolarization of the mitochondrial membrane, and increased the apoptosis rate (Figure 3I–L; supplementary material, Figure S4). In contrast, these effects were partially reversed by Sfn, an activator of Nrf2 signalling, or cobalt protoporphyrin IX (CoPP), a potent HO-1 inducer (Figure 3I–L; supplementary material, Figure S4).
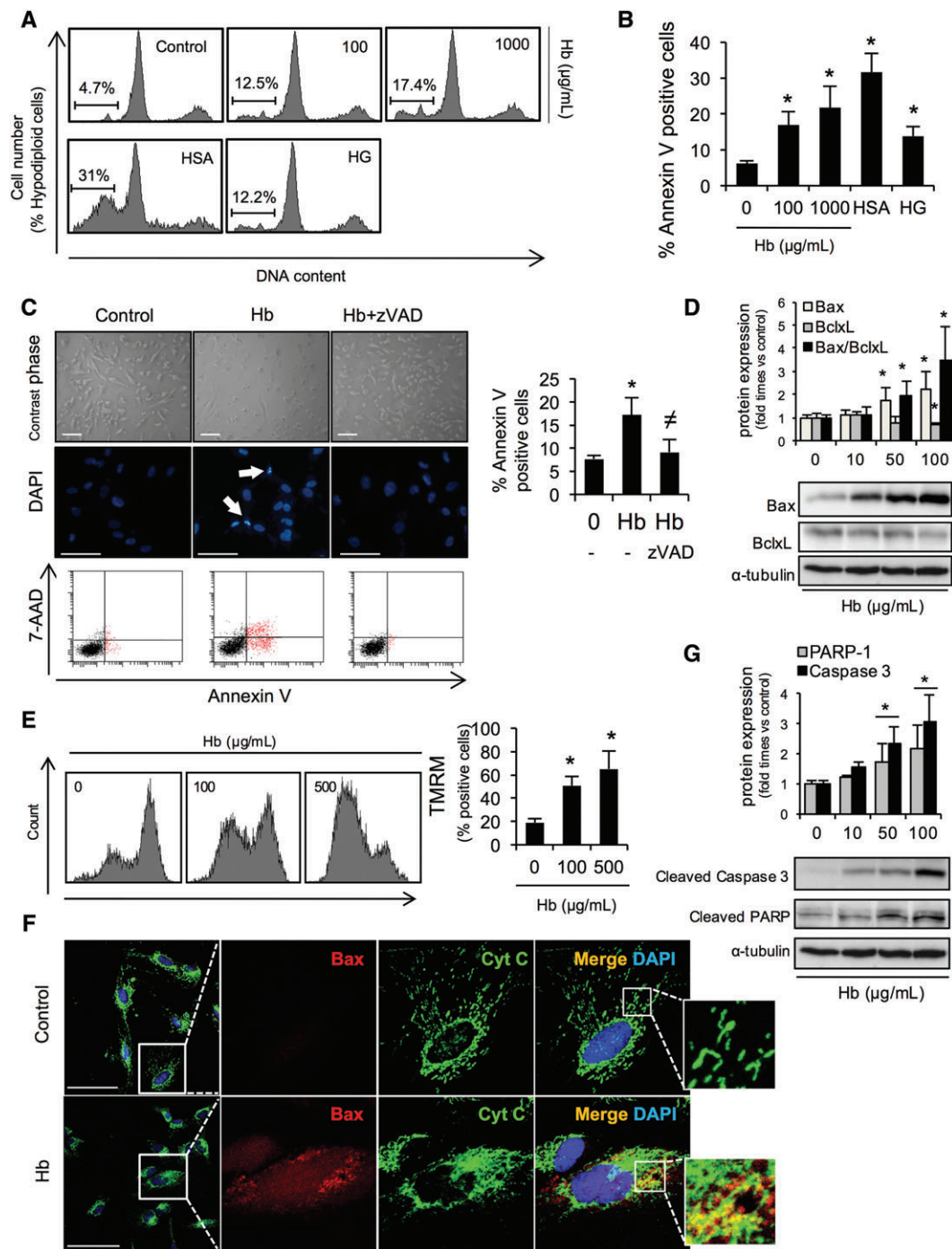
Figure 2. Hb induces apoptosis in cultured human podocytes. (A) Podocytes were cultured for 48 h in the presence of Hb (100–1000 µg/ml) for assessment of apoptosis by flow cytometry analysis of the cell cycle with propidium iodide. High glucose (HG, 25 mM) and HSA (50 mg/ml) were used as positive controls. (B) Cells were also stained with annexin V/7-AAD to confirm Hb-induced apoptosis. The graph shows averaged data of the apoptotic population (percentage of annexin V$^+$/7-AAD$^-$ and annexin V$^+$/7-AAD$^+$ cells) for each stimulus. (C) Representative contrast phase images showing a low number of attached viable cells and reduced cell size (upper panel), as well as shrunken, pyknotic and fragmented nuclei (arrows), in 4′,6-diamidino-2-phenylindole (DAPI)-stained cells exposed to Hb for 24 h (middle panel). All of these effects were reversed after addition of the pan-caspase inhibitor zVAD (25 µM), suggesting the involvement of caspases in Hb-mediated apoptosis. The lower panel shows representative histograms (left) and quantification (right) of annexin V-positive cells after Hb stimulation (100 µg/ml) with or without zVAD. Scale bars: 50 µm. (D) Western blot showing intracellular Bax and BclxL contents and the Bax/BclxL ratio in cells stimulated with Hb for 24 h. (E) Changes in mitochondrial membrane potential were assessed by monitoring TMRM fluorescence by flow cytometry. Representative histograms (left panels) and quantification (right panel) of TMRM-positive podocytes stimulated with different Hb concentrations (0–500 µg/ml) for 24 h are shown. (F) Representative confocal images showing cytochrome c release (Cyt C, green) and Bax content (red) in podocytes stimulated with Hb for 24 h. Nuclei were stained with DAPI (blue). Note the punctate mitochondrial pattern in control cells and diffuse labelling in podocytes stimulated with Hb, indicating cytochrome c release. Scale bar: 100 µm. The rectangle shows the region of interest for which high-magnification images are shown in the right panels. (G) Western blot showing caspase-3 activation and PARP-1 cleavage in podocytes stimulated with Hb for 24 h. (D) and (G) share the same tubulin panel. Results are expressed as mean ± SD of four independent experiments. *$p < 0.05$ versus non-stimulated cells; $^{\neq}p < 0.05$ versus Hb-stimulated cells.
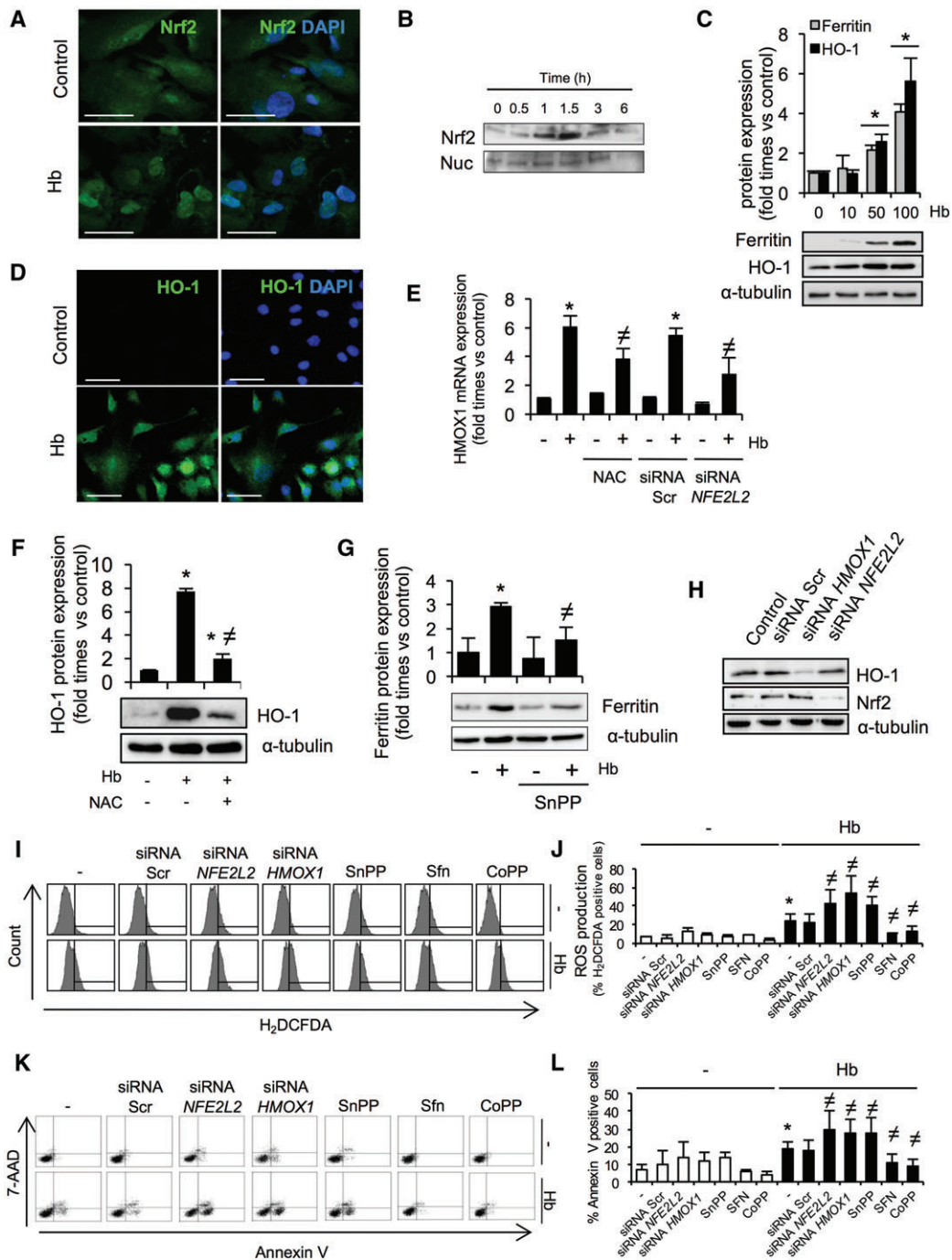
Figure 3. Hb activates the Nrf2–HO-1 pathway to promote intracellular haem catabolism and to reduce oxidative stress and apoptosis in cultured human podocytes. (A) Immunofluorescence images showing nuclear translocation of Nrf2 (green) in podocytes stimulated with Hb for 1 h. Nuclei were stained with 4′,6-diamidino-2-phenylindole (DAPI) (blue). Scale bars: 50 μm. (B) Nuclear translocation of Nrf2 was confirmed by western blotting of nuclear extracts (Nuc, nucleolin) obtained from podocytes stimulated with Hb at different time points. (C) Hb increased HO-1 and ferritin expression in a concentration-dependent manner as determined by western blotting (24 h). (D) Representative confocal images showing increased HO-1 expression (green) in podocytes stimulated with Hb for 24 h. Nuclei were stained with DAPI (blue). Scale bars: 50 μm. (E) *HMOX1* (HO-1) mRNA expression in podocytes that were pretreated for 1 h with NAC (1 mM) or were transfected with specific *NFE2L2* (Nrf2) siRNAs or scrambled (Scr) siRNA before Hb stimulation (100 μg/ml) for 6 h. (F) HO-1 expression in podocytes stimulated with Hb (100 μg/ml) for 24 h in the presence or absence of 1 mM NAC. (G) Ferritin expression in podocytes that were incubated with Hb (100 μg/ml) for 24 h in the presence or absence of a specific HO-1 inhibitor, SnPP (1 μM). Inhibition of ferritin synthesis by the HO-1 inhibitor SnPP demonstrates involvement of this enzyme in Hb catabolism in podocytes. In another set of experiments, podocytes were pretreated for 16 h with Sfn, an Nrf2 inducer (2 μM), and CoPP, an HO-1 activator (3 μM), or were transfected with specific *HMOX1* or *NFE2L2* siRNAs (25 nM). Podocytes were then incubated with Hb in the presence or absence of SnPP (1 μM) to determine ROS production and apoptosis by flow cytometry. (H) Representative western blot showing reduced HO-1 and Nrf2 expression in podocytes treated with *HMOX1*, *NFE2L2* or Scr siRNA. (I and J) Representative histograms (I) and quantification of ROS production (H_2DCFDA fluorescence intensity) (J) in podocytes stimulated with Hb for 3 h. (K and L) Representative histograms (K) and quantification of the percentage of annexin V-positive cells (early apoptotic plus late apoptotic/necrotic cells) (L) in podocytes stimulated with Hb for 48 h. Results are expressed as mean ± SD of four independent experiments. *$p < 0.05$ versus non-treated cells; ≠$p < 0.05$ versus Hb-stimulated cells.

Intravascular haemolysis promotes podocyte injury in an Nrf2-dependent way

To determine whether severe haemolysis promotes podocyte injury *in vivo*, we injected Phe into Nrf2$^{+/+}$ and Nrf2$^{-/-}$ mice. Severe haemolytic anaemia was observed after Phe administration, as shown by a reduced haematocrit and a reduced erythrocyte count, and by increased plasma and urine Hb concentrations, in both Nrf2$^{+/+}$ and Nrf2$^{-/-}$ mice (Table 2). However, no significant differences were observed according to Nrf2 genotype. Phe increased the urinary albumin/creatinine ratio, which is a marker of glomerular damage, although this effect was significantly more pronounced in Nrf2$^{-/-}$ mice (Table 2). Moreover, we found a positive correlation between urinary Hb levels and the urinary albumin/creatinine ratio ($r = 0.74$, $p < 0.05$).

Hb-loaded podocytes were observed during haemolysis in both Nrf2$^{+/+}$ and Nrf2$^{-/-}$ mice (Figure 4A); however, phosphorylated Nrf2 (pNrf2), HO-1 and ferritin staining was mainly observed in podocytes of wild-type mice (Figure 4A, B; supplementary material, Figure S5). Haemolysis induced podocyte apoptosis, as assessed by M30 staining, which is a specific marker of caspase activity [39] (Figure 4C, D). In line with this, a reduced podocyte number was observed in Phe-treated mice (Figure 4E, F). Transmission electron microscopy confirmed the presence of podocyte injury in these mice, as shown by podocyte foot process fusion or effacement (Figure 4G). Haemolysis decreased mRNA and protein levels of nephrin and synaptopodin, but increased urinary nephrin levels (Figure 4H–J). All of these pathological responses were increased in Phe-injected Nrf2$^{-/-}$ mice. The urinary Hb concentration was positively correlated with urinary nephrin levels ($r = 0.080$, $p < 0.01$) and M30 staining ($r = 0.079$, $p < 0.01$), and negatively correlated with glomerular nephrin expression ($r = -0.53$, $p < 0.05$) and podocyte number ($r = -0.43$, $p < 0.05$).

Nrf2 activation diminished podocyte injury during haemolysis

We further investigated whether administration of the Nrf2 inducer Sfn protected podocytes from haemolysis-induced damage. Although haemolysis did not change substantially in Sfn-treated mice, this compound reduced the urinary albumin/creatinine ratio in mice with haemolysis (Table 3). Sfn treatment promoted glomerular Nrf2 activation and induced glomerular HO-1 and ferritin expression, whereas it reduced M30 glomerular staining, fusion of podocyte foot processes and podocyte loss in Phe-treated mice (Figure 5A–G). Nrf2 induction also increased nephrin and synaptopodin glomerular expression, but reduced the urinary nephrin concentration (Figure 5H–J). These results support the notion that Nrf2 activation is effective in preventing haemolysis-mediated podocyte injury.

Podocytes from patients with intravascular haemolysis are damaged and show Hb accumulation

To determine whether Hb is incorporated by podocytes in human disease, we studied kidney biopsies from patients with intravascular haemolysis-associated AKI, caused by aHUS or severe transfusion reactions. Transmission electron microscopy showed podocyte damage, as indicated by the presence of large intracellular vacuoles that showed electron-dense iron deposits (Figure 6A), and loss and fusion of podocyte foot processes with iron deposits in the glomerular basement membrane (Figure 6B). In these patients, podocytes showed Hb staining (Figure 6C) and HO-1 and ferritin expression (supplementary material, Figure S6), indicating Hb uptake and intracellular haem degradation. Moreover, podocytes showed pNrf2 staining in the nucleus, suggesting activation of this transcription factor (Figure 6C). These markers were not observed in podocytes from healthy renal tissue.

Hb-rich podocytes are present in the urine of aHUS and PNH patients

Injured podocytes may detach from the glomerular tuft, so we investigated whether Hb uptake might induce podocyte loss. To this end, we performed immunofluorescence studies in urine sediments of subjects with active and severe haemolysis, such as aHUS and PNH. Urinary podocytes from aHUS patients showed intracellular and membrane Hb aggregates that were not present in podocytes from healthy individuals (Figure 6D). Hb-loaded podocytes were also seen in PNH patients (supplementary material, Figure S7).

Discussion

We have demonstrated, for the first time, that podocytes bind and endocytose Hb *in vitro* and *in vivo*, resulting in increased oxidative stress and apoptosis, and decreased expression of important functional and structural proteins of these cells (supplementary material, Figure S8). Moreover, Nrf2 activation prevents Hb toxicity in podocytes, and may therefore be a therapeutic target to decrease Hb-induced renal damage. Overall, our findings establish a new link between massive and persistent intravascular haemolysis, free Hb and podocyte injury that may explain the progressive impairment of renal function associated with this pathological setting. This novel concept opens the way for novel nephroprotective strategies for intravascular haemolysis-related diseases.

Independently of the cause, excessive intravascular haemolysis promotes Hb accumulation in the kidney [3] and renal damage [1,40,41]. Up to now, tubular cells have been considered to be the only sites for Hb toxicity. However, our results indicate that podocytes may also incorporate Hb. In agreement with our data, iron accumulated in podocytes from SCD patients
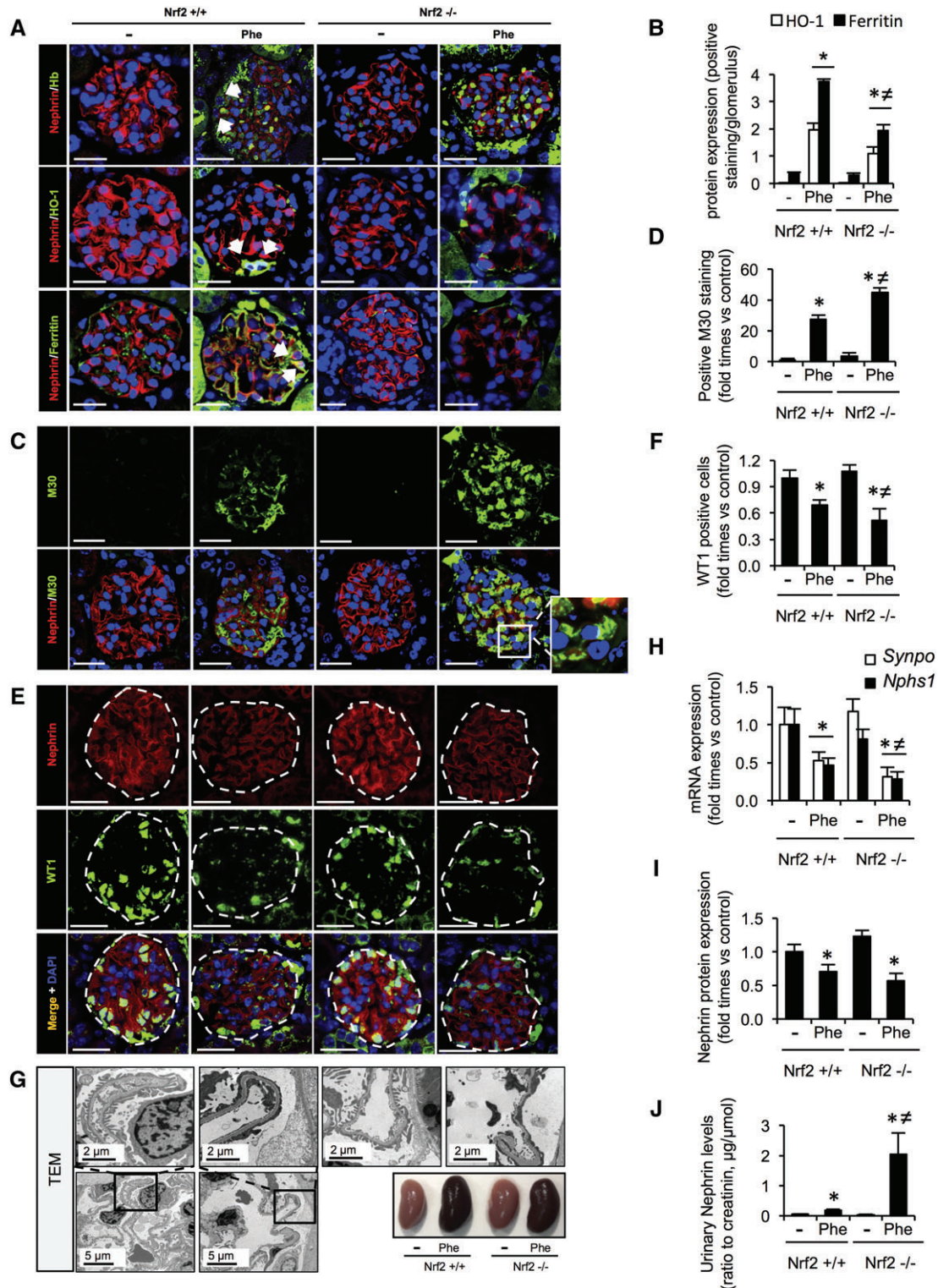
Figure 4. Intravascular haemolysis induces podocyte injury in an Nrf2-dependent way. Nrf2$^{+/+}$ or Nrf2$^{-/-}$ mice were injected with saline (-) or phenylhydrazine (Phe) to induce intravascular haemolysis ($n = 5$/group). (A) Representative confocal microscopy images showing co-localization (white arrows) of Hb (green), HO-1 (green) and ferritin (green) with the podocyte marker nephrin (red) in mice. Nuclei were stained with 4′,6-diamidino-2-phenylindole (DAPI) (blue). Scale bar: 25 μm. (B) Semi-quantification of HO-1 and ferritin positive staining per glomerular cross-section. (C–F) Immunofluorescence images (C and E) and semi-quantification (D and F) of M30 positive staining (green) and podocyte number [Wilms tumour-1 (WT1)-positive cells, green] per glomerular cross-section, respectively. Results are expressed as fold time increase as compared with control mice. The podocyte marker nephrin (red) was used to delimit the glomerular area. Nuclei were stained with DAPI (blue). Scale bar: 25 μm. (G) Representative transmission electron microscopy (TEM) images showing fusion of podocyte foot processes in Phe-treated mice. A representative kidney from each group is shown in the lower panel. (H and I) *Synpo* and *Nphs1* mRNA and nephrin protein expression measured by RT-qPCR and immunohistochemistry, respectively. (J) Urinary nephrin concentration determined by ELISA. Results were normalized to urinary creatinine levels, and are expressed as mean ± SEM. *$p < 0.05$ versus saline-treated mice; $^{\neq}p < 0.05$ versus Phe-treated Nrf2$^{+/+}$ mice.
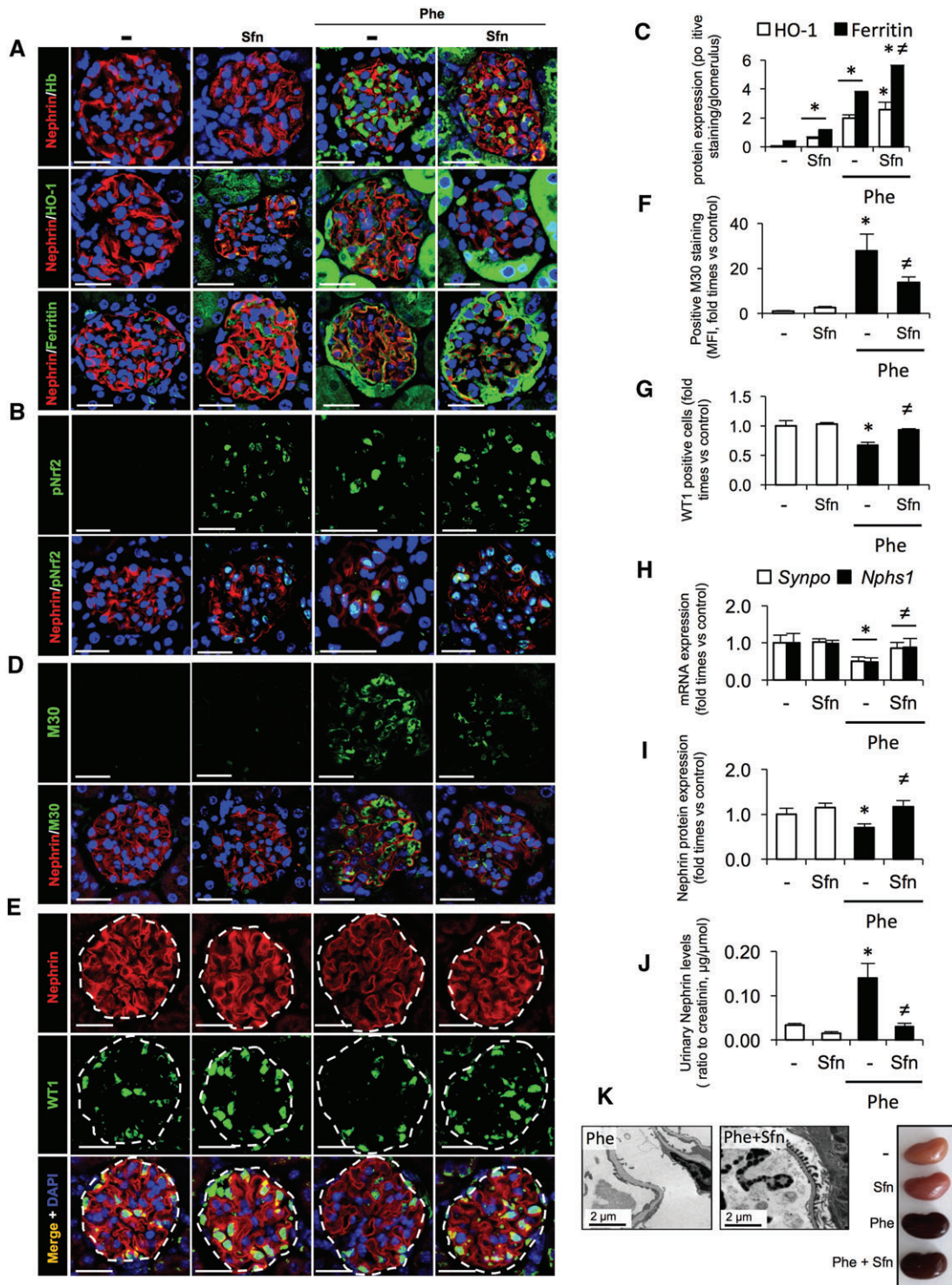
Figure 5. Amelioration of haemolysis–associated podocyte injury by Nrf2 activation. Sfn (12.5 mg/kg) was administered intraperitoneally 48, 24 and 2 h before Phe or saline injection in C57BL/6 mice ($n = 5$/group). (A and B) Representative confocal microscopy images showing Hb (green), HO-1 (green) and ferritin (green) expression (A) or nuclear pNrf2 staining (green) (B) in podocytes (nephrin-positive cells, red). Scale bar: 25 μm. Nuclei were stained with 4′,6-diamidino-2-phenylindole (DAPI) (blue). (C) Semi-quantification of HO-1 and ferritin positive staining per glomerular cross-section. (D–G) Immunofluorescence images (D and E) and semi-quantification (F and G) of M30 positive staining (green) and podocyte number [Wilms tumour-1 (WT1)-positive cells, green] per glomerular cross-section. Results are expressed as fold time increase as compared with control mice. The podocyte marker nephrin (red) was used to delimit the glomerular area. Nuclei were stained with DAPI (blue). Scale bar: 25 μm. (H and I) *Synpo* and *Nphs1* mRNA and nephrin protein expression measured by RT-qPCR and immunohistochemistry, respectively. (J) Urinary nephrin concentration determined by ELISA. Results were normalized to creatinine levels. (K) Representative transmission electron microscopy images showing less fusion of podocyte foot processes in Sfn-treated haemolytic mice. Scale bar: 2 μm. A representative kidney from each group is shown in the right panel. Results are expressed as mean ± SEM. *$p < 0.05$ versus saline-treated mice; ≠$p < 0.05$ versus saline-treated Phe mice. MFI, mean fluorescence intensity.
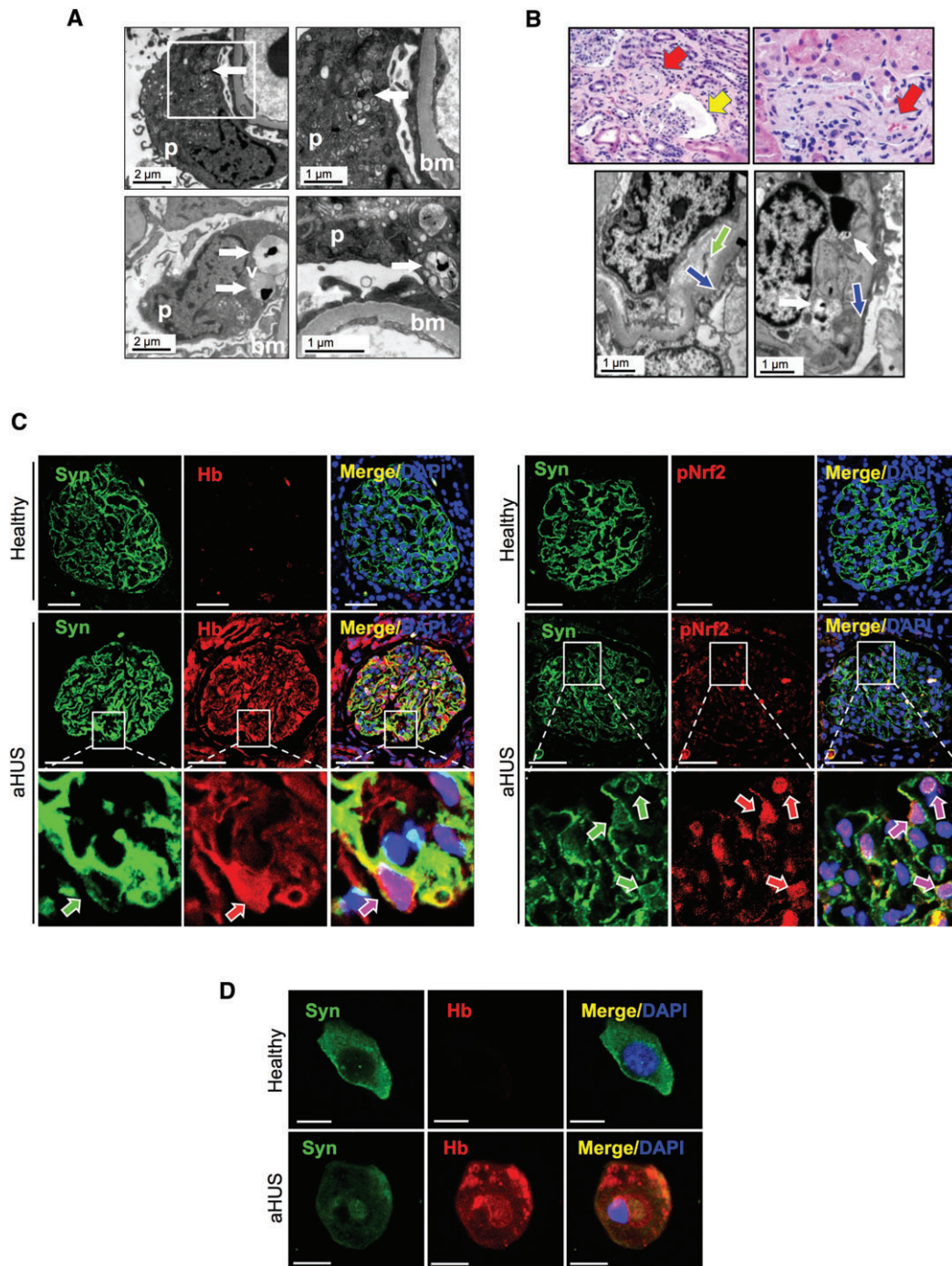
Figure 6. Uptake of Hb and activation of the haem degradation pathway in podocytes from patients with aHUS. (A) Electron micrographs showing podocytes (p) and adjacent basal membrane (bm) in the renal biopsy of a patient with haemolytic anaemia and AKI secondary to a severe transfusion reaction. The images show the presence of large podocyte vacuoles (v) with deposits of electron-dense iron (white arrows). The rectangle shows the region of interest for which a high-magnification image is shown in the upper right panel. (B) Representative haematoxylin and eosin staining in the renal biopsy from patients with aHUS-associated AKI showing ischaemic and sclerosed glomeruli (yellow arrow), with intracapillary erythrocyte fragmentation (red arrow), as well as generalized tubular atrophy, thickening of tubular basal membranes, and interstitial fibrosis (upper panel, left). The right panel shows vessels with concentric myointimal proliferation, luminal occlusion, and erythrocytes trapped within the vascular wall (red arrow). Electron micrographs of the renal biopsy of a patient with haemolytic anaemia and AKI secondary to aHUS show the presence of endothelial oedema (green arrow), loss and fusion of podocyte foot processes (blue arrows) and deposits of electron-dense iron (white arrows) in the glomerular basement membrane (lower panel). (C) Representative confocal microscopy images showing co-localization (white arrows) of Hb (red) and pNrf2 (red) with the podocyte marker synaptopodin (Syn, green) in patients with aHUS and healthy controls. Scale bars: 50 μm. Nuclei were stained with 4′,6-diamidino-2-phenylindole (DAPI) (blue). The rectangle shows the region of interest for which high-magnification images are shown in the lower panels. Scale bars: 10 μm. (D) Urine sediments from both healthy individuals and aHUS patients were centrifuged onto polylysine-coated slides with a cytospin, and immunofluorescence studies were then performed. Hb (red) was located inside podocytes (Syn-positive cells, green) from urine sediments of aHUS patients, as determined by confocal microscopy. DAPI (blue) was used to stain nuclei. Scale bars: 10 μm.

Table 2. Biochemical and haematological characteristics of Nrf2$^{+/+}$ and Nrf2$^{-/-}$ mice treated with Phe or saline

| | Nrf2$^{+/+}$ | | Nrf2$^{-/-}$ | | |
	Saline	Phe	Saline	Phe	P
Serum creatinine (mg/dl)	0.20 ± 0.03	0.30 ± 0.04*	0.23 ± 0.02	0.45 ± 0.05*,†,‡	<0.05
BUN (mg/dl)	31.42 ± 1.54	48.08 ± 2.76*	23.33 ± 1.47	56.42 ± 9.01*,‡	<0.001
Haematocrit (%)	49.99 ± 2.76	33.96 ± 3.51*	46.60 ± 1.68	31.25 ± 2.77‡	<0.05
Erythrocytes (10^6 cells/µl)	9.78 ± 0.37	7.21 ± 0.31*	10.12 ± 0.26	7.01 ± 0.50‡	<0.001
Serum Hb (g/dl)	15.74 ± 0.28	27.38 ± 4.32*	15.44 ± 0.69	25.86 ± 1.15‡	<0.05
Urinary albumin/creatinine ratio (µg/µmol)	8.53 ± 1.44	41.72 ± 11.20*	5.98 ± 1.24	109.21 ± 33.43*,†,‡	<0.001
Urinary Hb (µg/ml)	0.35 ± 0.13	3.40 ± 0.74*	0.29 ± 0.07	3.79 ± 1.40*,‡	<0.001

BUN, blood urea nitrogen.
Results are expressed as mean ± SEM.
*$p < 0.05$ versus saline-treated Nrf2$^{+/+}$ mice.
†$p < 0.05$ versus Phe-treated Nrf2$^{+/+}$ mice.
‡$p < 0.05$ versus saline-treated Nrf2$^{-/-}$ mice.

Table 3. Biochemical and haematological parameters in Sfn-treated and saline-treated Nrf2$^{+/+}$ mice with intravascular haemolysis

| | Control | | Phe | | |
	Saline	Sfn	Saline	Sfn	P
Serum creatinine (mg/dl)	0.13 ± 0.01	0.15 ± 0.02	0.26 ± 0.02*	0.21 ± 0.01*	<0.05
BUN (mg/dl)	33.66 ± 1.76	30.80 ± 0.9	46.16 ± 6.88*	39.25 ± 1.79*,†	<0.001
Haematocrit (%)	45.29 ± 4.17	51.75 ± 3.51	27.19 ± 1.50*	27.69 ± 0.04*	<0.05
Erythrocytes (10^6 cells/µl)	9.18 ± 0.88	10.56 ± 0.33	6.04 ± 0.22*	6.33 ± 0.09*	<0.001
Serum Hb (g/dl)	16.00 ± 1.26	17.95 ± 0.47	23.02 ± 1.03*	23.34 ± 1.77*	<0.05
Urinary albumin/creatinine ratio (µg/µmol)	8.45 ± 1.28	8.27 ± 1.70	34.81 ± 13.17*	14.02 ± 2.03*,†	<0.001
Urinary Hb (µg/ml)	0.31 ± 0.21	0.96 ± 0.11	3.71 ± 1.42*	3.23 ± 0.54*	<0.001

BUN, blood urea nitrogen.
Results are expressed as mean ± SEM.
*$p < 0.05$ versus control mice treated with saline or Sfn.
†$p < 0.05$ versus saline-treated Phe mice.

[21]. Careful examination of well-characterized human PNH and warm antibody haemolytic anaemia biopsies, published with a focus on tubular injury, also revealed ferritin in glomerular cells, probably podocytes [19,42]. We have demonstrated that Hb uptake by podocytes is an energy-dependent, active process mediated by the megalin–cubilin receptor system, which is expressed in podocytes [22,23], and constitutes the principal mechanism for Hb uptake in tubular epithelial cells [4]. Therefore, podocytes could be cellular targets for Hb toxicity in intravascular haemolysis. In this regard, disturbed podocyte morphology and podocyte necrosis were reported in experimental pre-eclampsia, characterized by intravascular haemolysis, proteinuria, and renal damage [43]. Moreover, podocyte foot process effacement and nephrotic-range proteinuria were described in diverse forms of aHUS [44–46]. In fact, nephrotic-range proteinuria can be seen in aHUS [13]. Although additional factors for podocyte injury may be invoked in some of the above-mentioned diseases, nephrotic-range proteinuria may also occur in non-microangiopathic intravascular haemolytic anaemias, such as PNH [47] and SCD [14], highlighting a potential relationship between massive haemolysis and glomerular dysfunction. Oxidative stress is a key trigger of podocyte injury, contributing to podocyte loss and proteinuria [34]. Hb is a potent generator of ROS [48], and increased ROS production has been observed in experimental models of podocyte injury [49]. We observed that Hb increased oxidative stress by increasing ROS production (superoxide anion and hydrogen peroxide) and

decreasing the level of GSH, the main water-soluble cellular antioxidant. Hb mediated ROS overproduction by NADPH oxidase, an enzyme that is highly expressed in podocytes [31]. Oxidative stress promotes podocyte apoptosis [34], which is an active response to injurious factors. In our study, Hb induced podocyte apoptosis *in vitro* and in haemolytic mice. Apoptosis is triggered by the activation of diverse signalling pathways. In the mitochondrial pathway (intrinsic pathway), pro-apoptotic Bax migrates to the mitochondrial membrane. Our results show that Hb upregulated Bax, downregulated anti-apoptotic BclxL, and promoted depolarization of the mitochondrial membrane and cytochrome c release in podocytes. Cytochrome c release leads to the sequential activation of effector caspases, such as caspase-3, which is the main caspase responsible for apoptotic cell death [35], and promotes cleavage of PARP-1, a protein that is necessary for cell survival [36]. In podocytes, Hb triggered caspase-3 activation and PARP-1 cleavage, and pretreatment with zVAD, a pan-caspase inhibitor, prevented Hb-mediated apoptosis, suggesting the involvement of caspases in Hb-induced podocyte death. These molecular mediators have also been shown to be involved in Hb-mediated tubular cell apoptosis [4]. The identification of molecular pathways for Hb-induced podocyte death highlights potential targets for molecular intervention to protect podocytes during intravascular haemolysis.

Podocytes are highly differentiated cells, with a specific cell structure underlying their function [17]. Podocyte injury is typically associated with

morphological changes, such as cell hypertrophy, actin cytoskeleton rearrangement, and foot process effacement, leading to podocyte detachment and loss [50]. In this regard, Hb altered podocyte morphology and deranged cytoskeletal actin filaments. Hb also decreased the expression of nephrin and synaptopodin, two multifunctional proteins that maintain the structural integrity of slit diaphragm and glomerular filtration function [33]. Our *in vivo* data confirmed the existence of podocyte injury, podocyte loss and downregulation of these slit diaphragm proteins during haemolysis. Dysregulation of these molecules represents a crucial event in the development of proteinuria in glomerular disease [17,33]. However, whether these molecules may serve as biomarkers of podocyte damage in haemolytic disorders is not yet known.

Nrf2 plays a pivotal role in the cellular defence against oxidative stress [7]. Under normal conditions, Nrf2 is bound to its cytosolic repressor Keap1, promoting its degradation via the proteasome [51]. However, stress signals modify Keap1 affinity for Nrf2, allowing Nrf2 nuclear translocation, as we observed in podocytes following Hb stimulation or in mice with intravascular haemolysis. Nrf2 was activated in different glomerular disorders [52], resulting in increased expression of antioxidant enzymes [51]. In line with this, Hb increased the expression of Nrf2-regulated genes, such as *HMOX1*, *NQO1*, *CAT*, and *TXNIP*, which, together, may protect against Hb-mediated oxidative stress [51]. Renal HO-1 expression is increased in Hb-derived nephropathies [3,19,42,53]. Moreover, examination of published images indicated that glomerular HO-1 may locate to podocytes in warm antibody haemolytic anaemia [19]. We observed HO-1, ferritin and pNrf2 staining in podocytes from renal sections of aHUS patients, supporting the translational significance of our findings. HO-1 may be induced by a number of oxidant stimuli, including Hb [37]. Moreover, HO-1 directly upregulates ferritin to store intracellular free iron produced by HO-1 catabolism [38]. Therefore, the increased ferritin expression observed in Hb-treated podocytes suggests that HO-1 induction was directly associated with Hb uptake. Besides Nrf2, HO-1 is upregulated by other transcription factors, such as activator protein-1 and heat shock factor [54]. This fact may explain why Nrf2 targeting reduced Hb-mediated HO-1 induction in podocytes.

Accumulating lines of evidence support the protective role of Nrf2 against oxidative stress in renal injury [55]. Nrf2 induction reduced podocyte damage in different animal models, including focal segmental glomerulosclerosis, crescentic glomerulonephritis, and membranous nephropathy [55]. Nrf2 activation decreased liver damage and lung inflammation in experimental models of SCD [56]. However, there are no studies supporting a protective role of Nrf2 in Hb-mediated renal injury. Our data obtained in Nrf2-deficient mice showed that the lack of Nrf2 increased proteinuria and podocyte injury during haemolysis, whereas Nrf2 activation had a beneficial effect. Similarly, Nrf2 and HO-1 targeting increased Hb-mediated oxidative stress and apoptosis in cultured podocytes. Altogether, these results suggest that Nrf2 activation may be effective in preventing haemolysis-mediated podocyte injury. It is important to note that sustained systemic Nrf2 induction may be toxic and lead to a higher risk of cancer, whereas transient and mild Nrf2 activation is probably beneficial [57]. Recent studies have indicated that the protective effects of Nrf2 on the kidney are observed at low activation levels, whereas harmful effects appear at higher activation levels [55]. These observations might indicate that precise administration of Nrf2 inducers may be protective; however, the specific doses must be determined carefully.

In conclusion, our study identifies podocytes as new cellular targets of Hb-derived toxicity in pathologies characterized by increased intravascular haemolysis. Podocyte injury may result from Hb endocytosis, increased oxidative stress, and apoptosis, as well as reduced expression of the slit diaphragm proteins. These effects may explain the progressive impairment of renal function observed in these pathologies. Moreover, activation of the Nrf2 pathway may be a powerful therapeutic strategy to prevent Hb-mediated podocyte injury. These findings provide new insights into novel aspects of Hb toxicity in the kidney, and may have important pathogenic and therapeutic implications for renal damage associated with massive intravascular haemolysis.

Acknowledgements

Author contributions statement

The authors contributed in the following way: ARN, JAM: designed the study; AMS, CY, ER: were involved in human sample collection; PC, RO: analysed renal biopsies; ARN, MDSN, MGH, SC, MG, IC, CGC, BA: performed research; ARN, MGH, IC, JAM: performed

data analysis and data interpretation; EG, ARN, MDSN, JE, AO, MP, ER, JAM: wrote the manuscript. All authors critically revised the manuscript for important intellectual content.

References

1. Moreno JA, Martin-Cleary C, Gutierrez E, *et al.* AKI associated with macroscopic glomerular hematuria: clinical and pathophysiologic consequences. *Clin J Am Soc Nephrol* 2012; **7:** 175–184.

2. Naik RP, Derebail VK, Grams ME, *et al.* Association of sickle cell trait with chronic kidney disease and albuminuria in African Americans. *JAMA* 2014; **312:** 2115–2125.

3. Ballarin J, Arce Y, Torra BR, *et al.* Acute renal failure associated to paroxysmal nocturnal haemoglobinuria leads to intratubular haemosiderin accumulation and CD163 expression. *Nephrol Dial Transplant* 2011; **26:** 3408–3411.

4. Tracz MJ, Alam J, Nath KA. Physiology and pathophysiology of heme: implications for kidney disease. *J Am SocNephrol* 2007; **18:** 414–420.

5. Stocker R. Induction of haem oxygenase as a defence against oxidative stress. *Free Radic Res Commun* 1990; **9:** 101–112.

6. Nath KA. Heme oxygenase-1: a provenance for cytoprotective pathways in the kidney and other tissues. *Kidney Int* 2006; **70:** 432–443.

7. Wakabayashi N, Slocum SL, Skoko JJ, *et al.* When NRF2 talks, who's listening? *Antioxid Redox Signal* 2010; **13:** 1649–1663.

8. Nath KA, Croatt AJ, Haggard JJ, *et al.* Renal response to repetitive exposure to heme proteins: chronic injury induced by an acute insult. *Kidney Int* 2000; **57:** 2423–2433.

9. De Paepe ME, Trudel M. The transgenic SAD mouse: a model of human sickle cell glomerulopathy. *Kidney Int* 1994; **46:** 1337–1345.

10. Falk RJ, Scheinman J, Phillips G, *et al.* Prevalence and pathologic features of sickle cell nephropathy and response to inhibition of angiotensin-converting enzyme. *N Engl J Med* 1992; **326:** 910–915.

11. Caletti MG, Gallo G, Gianantonio CA. Development of focal segmental sclerosis and hyalinosis in hemolytic uremic syndrome. *PediatrNephrol* 1996; **10:** 687–692.

12. Fremeaux-Bacchi V, Fakhouri F, Garnier A, *et al.* Genetics and outcome of atypical hemolytic uremic syndrome: a nationwide French series comparing children and adults. *Clin J Am SocNephrol* 2013; **8:** 554–562.

13. Noris M, Mele C, Remuzzi G. Podocyte dysfunction in atypical haemolytic uraemic syndrome. *Nat Rev Nephrol* 2015; **11:** 245–252.

14. Pham PT, Pham PC, Wilkinson AH, *et al.* Renal abnormalities in sickle cell disease. *Kidney Int* 2000; **57:** 1–8.

15. Schmitt F, Martinez F, Brillet G, *et al.* Early glomerular dysfunction in patients with sickle cell anemia. *Am J Kidney Dis* 1998; **32:** 208–214.

16. Moreno JA, Sanchez-Nino MD, Sanz AB, *et al.* A slit in podocyte death. *Curr Med Chem* 2008; **15:** 1645–1654.

17. Pavenstadt H, Kriz W, Kretzler M. Cell biology of the glomerular podocyte. *Physiol Rev* 2003; **83:** 253–307.

18. Tryggvason K, Patrakka J, Wartiovaara J. Hereditary proteinuria syndromes and mechanisms of proteinuria. *N Engl J Med* 2006; **354:** 1387–1401.

19. Fervenza FC, Croatt AJ, Bittar CM, *et al.* Induction of heme oxygenase-1 and ferritin in the kidney in warm antibody hemolytic anemia. *Am J Kidney Dis* 2008; **52:** 972–977.

20. De PL, Patrick J, Christen E, *et al.* Urinary podocyte mRNA excretion in children with D+HUS: a potential marker of long-term outcome. *Ren Fail* 2006; **28:** 475–482.

21. Elfenbein IB, Patchefsky A, Schwartz W, *et al.* Pathology of the glomerulus in sickle cell anemia with and without nephrotic syndrome. *Am J Pathol* 1974; **77:** 357–374.

22. Prabakaran T, Christensen EI, Nielsen R, *et al.* Cubilin is expressed in rat and human glomerular podocytes. *Nephrol Dial Transplant* 2012; **27:** 3156–3159.

23. Prabakaran T, Nielsen R, Larsen JV, *et al.* Receptor-mediated endocytosis of alpha-galactosidase A in human podocytes in Fabry disease. *PLoS One* 2011; **6:** e25065.

24. Saleem MA, O'Hare MJ, Reiser J, *et al.* A conditionally immortalized human podocyte cell line demonstrating nephrin and podocin expression. *J Am SocNephrol* 2002; **13:** 630–638.

25. Sastre C, Rubio-Navarro A, Buendia I, *et al.* Hyperlipidemia-associated renal damage decreases Klotho expression in kidneys from ApoE knockout mice. *PLoS One* 2013; **8:** e83713.

26. Kamencic H, Lyon A, Paterson PG, *et al.* Monochlorobimane fluorometric method to measure tissue glutathione. *Anal Biochem* 2000; **286:** 35–37.

27. Ryter SW, Kvam E, Tyrrell RM. Heme oxygenase activity. Current methods and applications. *Methods Mol Biol* 2000; **99:** 369–391.

28. Moreno JA, Izquierdo MC, Sanchez-Nino MD, *et al.* The inflammatory cytokines TWEAK and TNFalpha reduce renal klotho expression through NFkappaB. *J Am Soc Nephrol* 2011; **22:** 1315–1325.

29. Rubio-Navarro A, Carril M, Padro D, *et al.* CD163-macrophages are involved in rhabdomyolysis-induced kidney injury and may be detected by MRI with targeted gold-coated iron oxide nanoparticles. *Theranostics* 2016; **6:** 896–914.

30. Vogelmann SU, Nelson WJ, Myers BD, *et al.* Urinary excretion of viable podocytes in health and renal disease. *Am J Physiol Renal Physiol* 2003; **285:** F40–F48.

31. Greiber S, Munzel T, Kastner S, *et al.* NAD(P)H oxidase activity in cultured human podocytes: effects of adenosine triphosphate. *Kidney Int* 1998; **53:** 654–663.

32. Hwang C, Sinskey AJ, Lodish HF. Oxidized redox state of glutathione in the endoplasmic reticulum. *Science* 1992; **257:** 1496–1502.

33. Welsh GI, Saleem MA. Nephrin-signature molecule of the glomerular podocyte? *J Pathol* 2010; **220:** 328–337.

34. Oba S, Hino M, Fujita T. Adrenomedullin protects against oxidative stress-induced podocyte injury as an endogenous antioxidant. *Nephrol Dial Transplant* 2008; **23:** 510–517.

35. Ortiz A. Nephrology forum: apoptotic regulatory proteins in renal injury. *Kidney Int* 2000; **58:** 467–485.

36. Kaufmann SH, Desnoyers S, Ottaviano Y, *et al.* Specific proteolytic cleavage of poly(ADP-ribose) polymerase: an early marker of chemotherapy-induced apoptosis. *Cancer Res* 1993; **53:** 3976–3985.

37. Sardana MK, Kappas A. Dual control mechanism for heme oxygenase: tin(IV)-protoporphyrin potently inhibits enzyme activity while markedly increasing content of enzyme protein in liver. *Proc Natl Acad Sci U S A* 1987; **84:** 2464–2468.

38. Berberat PO, Katori M, Kaczmarek E, *et al.* Heavy chain ferritin acts as an antiapoptotic gene that protects livers from ischemia reperfusion injury. *FASEB J* 2003; **17:** 1724–1726.

39. Santamaria B, Ucero AC, Reyero A, *et al.* 3,4-Dideoxyglucosone-3-ene as a mediator of peritoneal demesothelization. *Nephrol Dial Transplant* 2008; **23:** 3307–3315.

40. Moreno JA, Martin-Cleary C, Gutierrez E, *et al.* Haematuria: the forgotten CKD factor? *Nephrol Dial Transplant* 2012; **27:** 28–34.

41. Nair RK, Khaira A, Sharma A, *et al.* Spectrum of renal involvement in paroxysmal nocturnal hemoglobinuria: report of three cases and a brief review of the literature. *Int Urol Nephrol* 2008; **40:** 471–475.

42. Nath KA, Vercellotti GM, Grande JP, *et al.* Heme protein-induced chronic renal inflammation: suppressive effect of induced heme oxygenase-1. *Kidney Int* 2001; **59:** 106–117.

43. Wester-Rosenlof L, Casslen V, Axelsson J, *et al.* A1M/alpha1-microglobulin protects from heme-induced placental and renal

damage in a pregnant sheep model of preeclampsia. *PLoS One* 2014; **9**: e86353.

44. Lemaire M, Fremeaux-Bacchi V, Schaefer F, *et al.* Recessive mutations in DGKE cause atypical hemolytic-uremic syndrome. *Nat Genet* 2013; **45**: 531–536.

45. Ozaltin F, Li B, Rauhauser A, *et al.* DGKE variants cause a glomerular microangiopathy that mimics membranoproliferative GN. *J Am Soc Nephrol* 2013; **24**: 377–384.

46. Landau D, Shalev H, Levy-Finer G, *et al.* Familial hemolytic uremic syndrome associated with complement factor H deficiency. *J Pediatr* 2001; **138**: 412–417.

47. Hillmen P, Elebute M, Kelly R, *et al.* Long-term effect of the complement inhibitor eculizumab on kidney function in patients with paroxysmal nocturnal hemoglobinuria. *Am J Hematol* 2010; **85**: 553–559.

48. Jia Y, Buehler PW, Boykins RA, *et al.* Structural basis of peroxide-mediated changes in human hemoglobin: a novel oxidative pathway. *J Biol Chem* 2007; **282**: 4894–4907.

49. Shah SV, Baliga R, Rajapurkar M, *et al.* Oxidants in chronic kidney disease. *J Am Soc Nephrol* 2007; **18**: 16–28.

50. Patrakka J, Tryggvason K. New insights into the role of podocytes in proteinuria. *Nat Rev Nephrol* 2009; **5**: 463–468.

51. Jaiswal AK. Nrf2 signaling in coordinated activation of antioxidant gene expression. *Free Radic Biol Med* 2004; **36**: 1199–1207.

52. Henique C, Bollee G, Lenoir O, *et al.* Nuclear factor erythroid 2-related factor 2 drives podocyte-specific expression of peroxisome proliferator-activated receptor gamma essential for resistance to crescentic GN. *J Am Soc Nephrol* 2016; **27**: 172–188.

53. Garcia-Camin RM, Goma M, Osuna RG, *et al.* Molecular mediators of favism-induced acute kidney injury. *Clin Nephrol* 2014; **81**: 203–209.

54. Alam J, Cook JL. How many transcription factors does it take to turn on the heme oxygenase-1 gene? *Am J Respir Cell Mol Biol* 2007; **36**: 166–174.

55. Hue MG, Farré-Alins V, Antolin AP, *et al.* Targeting Nrf2 in the protection against renal disease. *Curr Med Chem* 2017; **24**: 3583–3605.

56. Keleku-Lukwete N, Suzuki M, Otsuki A, *et al.* Amelioration of inflammation and tissue damage in sickle cell model mice by Nrf2 activation. *Proc Natl Acad Sci U S A* 2015; **112**: 12169–12174.

57. Kensler TW, Wakabayashi N. Nrf2: friend or foe for chemoprevention? *Carcinogenesis* 2010; **31**: 90–99.

SUPPLEMENTARY MATERIAL ONLINE

Supplementary figure legends

Figure S1. Hb uptake by human podocytes

Figure S2. *Ex vivo* Hb uptake by murine podocytes promotes oxidative stress and activation of the Nrf2/HO-1 pathway

Figure S3. Hb promotes Nrf2-related gene expression in human podocytes

Figure S4. Effects of Nrf2 and HO-1 modulation on Hb-induced changes in mitochondrial membrane potential in cultured human podocytes

Figure S5. Nrf2 activation in phenylhydrazine-treated mice

Figure S6. HO-1 and ferritin expression in podocytes from patients with atypical hemolytic uremic syndrome

Figure S7. Hb-loaded podocytes in urine from patients with active paroxysmal nocturnal hemoglobinuria

Figure S8. Schematic representation of Hb-mediated toxicity in podocytes

Table S1. Gene expression assays used in the study

Table S2. Antibodies used in the study